

Granule transport and mean residence time in horizontal drum with inclined flights

Jian-Ping Pan, Ting-Jie Wang*, Jun-Jie Yao, Yong Jin

Beijing Key Laboratory of Green Reaction Engineering and Technology, Department of Chemical Engineering, Tsinghua University, Beijing 100084, China

Received 30 December 2004; received in revised form 12 October 2005

Abstract

Experiments on granule transport and the mean residence time in a rotary horizontal drum with inclined flights showed that the granules can be transported steadily. A model for granule transport based on the analysis of granule motion and other studies on inclined drums was developed to calculate the mean residence time of the granules, and verification experiments under different conditions were conducted. The calculations agreed well with experimental results. The variation of the mean residence time with feed rate, flight slope and rotation speed was modeled and compared with experimental results.

© 2005 Elsevier B.V. All rights reserved.

Keywords: Horizontal drum; Flight; Residence time; Granule; Transport

1. Introduction

Drums, flighted drums in particular, are widely used in granulation and granule drying or cooling [1]. In recent researches on a coated fertilizer for controlled/slow release, the drum is a key device in the coating granulation process [2]. Drum has shown many advantages such as a narrow distribution of residence time, wide operation range and broad applicability. In conventional drums, the flights are parallel to the axis of the drum. Thus, for granule transport, the conventional drum must be inclined, and the whole device and relevant parts have to be inclined. As a result, the construction is very complex, the installation and maintenance of the inclined drum are quite inconvenient, and device abrasion is serious, especially for a large size inclined drum. The problems of an inclined drum are much more obvious when the drum is very long or there are fixed inner structures [3]. Drums mounted horizontally with a smooth transport of the granules in the drum will not have many of the engineering problems that the inclined drum has.

Experiments have shown that axial granule transport is possible in rotary horizontal drum whose flights are inclined to

the generatrix of the drum wall. A rotary horizontal drum with inclined flights can transport granules like a conventional inclined drum, its installation and maintenance are convenient, and there will not be any problems with device abrasion and structure interference.

A lot of researches on the mean residence time of granules in conventional drums [1,4–7] and the effect of flights [8,9] have been reported. Using geometrical deduction and calculation, Saeman [4] gave the time of passage, axial transport velocity, bed depth and other characteristics related to the passage of material through a rotary drum without flights. Using the definition of the airborne phase and dense phase in drum by former researchers, Sherritt et al. [1] obtained the mean residence time of granules by calculating the holdup in the whole drum and the axial flow rate of granules in the airborne and the dense phase. Wang et al. [5–7] developed a non-equilibrium distributed parameter model for the rotary drying and cooling processes with a set of partial differential equations with nonlinear algebraic constraints, and investigated the residence time of the granules. Revol et al. [8] and Wang [9] studied holdup and the discharging process of flights by describing the relationship of flight, drum wall and exposed surface of the granule with an algebraic method.

However, there are few researches on horizontal drums with flights. Most of the studies have been on micro-dynamic

* Corresponding author. Tel.: +86 10 62788993; fax: +86 10 62772051.
E-mail address: wangtj@mail.tsinghua.edu.cn (T.-J. Wang).

analysis [10] or the segregation [11] of granules in horizontal drums without flights. No investigator has studied granule motion and residence time in horizontal drums with inclined flights. The residence time model of a conventional drum cannot be used directly for a horizontal drum, because a very important parameter, the drum slope, is zero, i.e. horizontal, and consequently, the calculated residence time will be infinity. In this paper, a simplified transport model for granules in a novel drum, namely a horizontal drum with inclined flights, is developed, and the mean residence time of granules is calculated with this model and compared with experimental results.

2. Model of granule transport in a flighted horizontal drum

2.1. Motion of granules in a drum

There are two possible loading states in a flighted drum, underloaded and overloaded. In an underloaded drum, the initial discharge flight is in the upper half of drum, i.e. $\varphi_{min} \geq 0$. In an overloaded drum, the initial discharge flight is in the lower half of the drum, i.e. $\varphi_{min} < 0$. This paper studied the underloaded situation in order to simplify the model and discussion. The cross section of an underloaded drum and the general state of the granules are shown in Fig. 1. Following the rotation of the drum, the granules are lifted by the flight. When the flight reaches a certain position, it begins to discharge the granules, i.e. the discharging process starts. The flight moves

with the drum and discharges continually, and the holdup of the flight reduces. The discharging process ends when all of the granules in the flight are discharged. The granules discharged from the flight fall into the bottom of drum, are lifted by the following flight and then enter the discharging process referred to before. The motion of the granules in the drum is the cycling of this “lifted–discharged” process. As a result of the inclination of the flights, when the granule is sliding in the flight or discharged, the direction of granule movement and the cross section of the drum form an included angle. This is the cause of the axial displacement of granules in the sliding and falling. After many such circulations, the granules pass through the drum. The model in this paper aims to describe the motion of the granules in one circulation. The mean axial displacement of all granules in one circulation is inferred from the model, and the mean residence time obtained.

Using the definition by former investigators [1], the granules in the drum are regarded as existing in two phases that are the airborne phase and dense phase. The dense phase consists of resting granules accumulated in flights and in the bottom of the drum, while the airborne phase consists of the falling granules discharged from the flights. Thus, the axial displacement of granules can be separated into an axial displacement which occurs in the dense phase Z_{dense} , and an axial displacement which occurs in the airborne phase Z_{air} . Similarly, the circulation time is separated into a residence time in the dense phase t_{dense} , and a residence time in the airborne phase t_{air} . The following expressions denote the axial

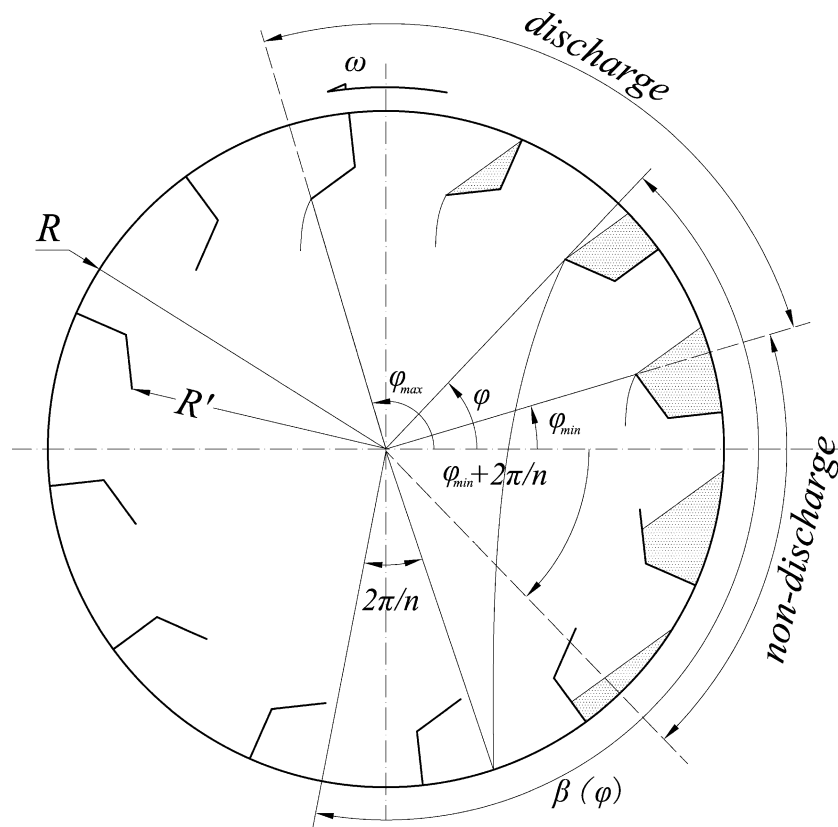


Fig. 1. Sketch of the drum cross section.

displacement and circulation time of the granule in one circulation,

$$\begin{cases} Z = Z_{\text{dense}} + Z_{\text{air}} \\ t = t_{\text{dense}} + t_{\text{air}} \end{cases} \quad (1)$$

The average speed of axial transfer \bar{U} can be expressed as below,

$$\bar{U} = \left(\frac{Z}{t} \right) \quad (2)$$

Assume the length of drum is L , the mean residence time τ is obtained:

$$\tau = L/\bar{U} \quad (3)$$

This is the basic concept of the mean residence time model.

Some basic assumptions are made in the analysis. In the discharging process, it is assumed that the surface granules in one flight discharge out at the same time, and the time for the granules to slide out of the flight is short and negligible. The slopes of the surface of piles of granules in any discharging flights are assumed the same and equal to the kinetic angle of repose of the granule. The axial displacement in the dense phase is assumed to consist of two parts, one in the sliding surface in flights when discharging and other in the non-discharge process of the dense phase. The latter is treated following the assumption of axis displacement in a non-discharge process by Sherritt et al. [1].

Some parameters for analyzing the granule motion are defined here. The azimuth of flight φ , shown in Fig. 1, is the included angle formed by the 0° horizontal line and the line connecting the circle center and tip of the flight, and the 0° horizontal line is the horizon which flights crossed from the lower half of the drum to the upper half when the drum rotates. At the start of the flight discharging process, the azimuth of flight is defined as φ_{min} ; at the end of the discharging process, the azimuth of flight is defined as, φ_{max} , as shown in Fig. 1. φ_{min} is affected by many conditions, such as the feed rate, rotary speed, flight geometry, and so on. φ_{max} , however, is almost just a function of the flight geometry and granules' property, the angle of repose. The drum radius is R , and n trains of flights are fixed in the drum. The slope of the flights relative to the generatrix of the drum wall is θ . Each flight is axially folded at an included angle α , and the widths of the two segments are b_1 and b_2 . According to the law of cosines, R' is obtained easily:

$$R' = \sqrt{(R - b_2)^2 + b_1^2 + 2b_1(R - b_2)\cos\alpha} \quad (4)$$

The kinetic angle of repose ψ is defined as the included angle formed by the exposed surface of the granules and the horizontal plane in the rotary drum. The variation of ψ with the rotary speed ω and the azimuth of flight φ is described as [9,12]:

$$\tan\psi = \frac{\mu + R' \frac{\omega^2}{g} (\cos\varphi - \mu\sin\varphi)}{1 - R' \frac{\omega^2}{g} (\sin\varphi + \mu\cos\varphi)} \quad (5)$$

In Eq. (5), μ is the coefficient of dynamic friction, and R' is the radius of the circle on which the tips of the flights are located. It is shown from calculations that the calculated ψ do not change much and the relative deviation of ψ is less than 10% when $R' < 1.5$ m, the rotary speed < 8 rpm and $\mu < \tan(30^\circ)$. The included angle formed by the line CD and line DO' , in Fig. 2, the intersection of the horizontal plane and the drum cross section, is not equal to the kinetic angle of repose ψ , and it is defined as ψ' . The length of the intersection of the drum cross section and the exposed surface of granules is l , shown in Fig. 3.

In a circulation, the range of motion of the granules in the dense phase β is defined as the angle range from where the granule enters the dense phase to where it is discharged from the flight. It should be mentioned that β of different granules may be different. γ is defined as the shift angle, which is the direction of sliding relative to the drum cross section when granules slide out from the flight. The shift angle γ induces the axial displacement of granules in discharging and falling.

Obviously, the length of the exposed surface of granules l is a function of the azimuth of flight φ , the kinetic angle of repose ψ , and structural parameters, such as α , b_1 , b_2 and R . In a specific drum at a fixed rotation velocity, the parameters other than the azimuth of flight φ and the kinetic angle of repose ψ are fixed. Under such a condition, there is only one variable, the azimuth of flight φ , in the function describing the kinetic angle of repose ψ . Thus, l is simplified into a function of φ .

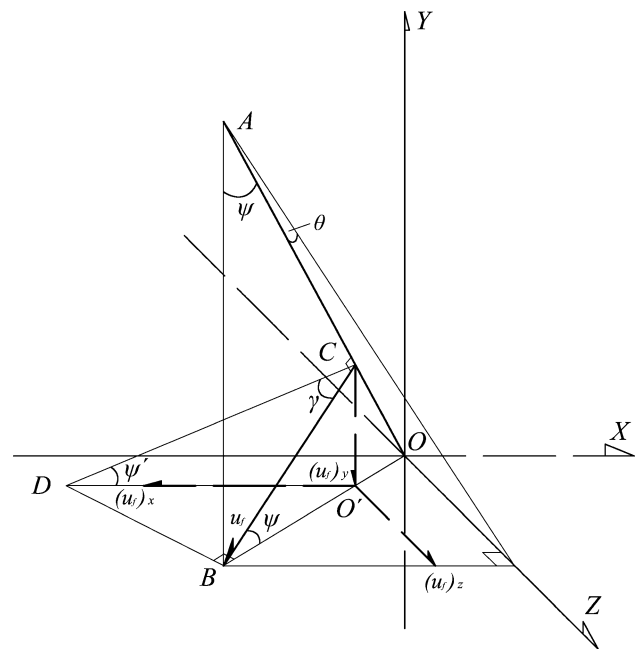


Fig. 2. Decomposition of the sliding velocity of the granules on the X , Y , Z coordinate axes. Note: Z is the direction of granules transfer along the axis of drum, which is horizontal, Y is vertically up, X is horizontal and perpendicular to the axis of the drum; OA is the normal of the exposed surface of granules, the included angle between OA and OXY is equal to the slope of flights θ ; C is the cross point of OA and plane of exposed surface; CB is the cross line of the plane of exposed surface and plane formed by OA and gravity direction, which is the direction of granule sliding velocity; D is in the plane of exposed surface; BD is perpendicular to the plane OAB ; and CD is in a vertical plane.

It is easy to derive that the expressions for the included angle ψ' and included angle γ are as shown in Eq. (15).

$$\begin{cases} \psi' = \arctan(\tan\psi \cdot \cos(\arcsin(\sin\theta/\sin\psi))) \\ \gamma = \arccos(\sin\psi'/\sin\psi) \end{cases} \quad (15)$$

Referring to Fig. 2, the components of u_f on the X , Y , Z coordinate axes are as shown below:

$$\begin{cases} (u_f)_x = -u_f \cdot (\cos\psi \cdot \sin\theta/\sin\psi) / \tan(\arcsin(\sin\theta/\sin\psi)) \\ (u_f)_y = -u_f \cdot \sin\psi \\ (u_f)_z = u_f \cdot \cos\psi \cdot \sin\theta/\sin\psi \end{cases} \quad (16)$$

Z is the direction of granule transfer along the axis of the drum, Y is vertically up, and X is horizontal and perpendicular to the axis of the drum. The granules in the flights are in circular motion with a rotary drum, so, a tangential velocity u_t exists. At the moment when granules are just discharged from the flight, the tangential velocity of the granules is denoted as $u_t = \omega R'$. As shown in Fig. 4, u_t has the following components on the three coordinate axes:

$$\begin{cases} (u_t)_x = -u_t \cdot \sin\varphi \\ (u_t)_y = u_t \cdot \cos\varphi \\ (u_t)_z = 0 \end{cases} \quad (17)$$

Therefore, the velocity of granules at the moment when the granules are just discharged from the flight is expressed as:

$$\begin{cases} u_x(\varphi) = -u_t \cdot \sin\varphi - u_f \cdot (\cos\psi \cdot \sin\theta/\sin\psi) / \tan(\arcsin(\sin\theta/\sin\psi)) \\ u_y(\varphi) = u_t \cdot \cos\varphi - u_f \cdot \sin\psi \\ u_z(\varphi) = u_f \cdot \cos\psi \cdot \sin\theta/\sin\psi \end{cases} \quad (18)$$

The initial position of falling granules (X_0, Y_0) is given by the following expression.

$$\begin{cases} X_0 = R' \cos\varphi \\ Y_0 = R' \sin\varphi \end{cases} \quad (19)$$

Thus, the position of granules falling by gravity can be described with the parameter equations related to the residence time in the airborne phase, t_{air} :

$$\begin{cases} X = X_0 + u_x t_{\text{air}}(\varphi) \\ Y = Y_0 + u_y t_{\text{air}} - \frac{1}{2} g \cdot (t_{\text{air}}(\varphi))^2 \end{cases} \quad (20)$$

When they arrive at the wall of the drum, granules enter the dense phase. The drum wall is described by the following equation:

$$X^2 + Y^2 = R^2 \quad (21)$$

By solving the simultaneous Eq. (20), describing the position of a falling granule, and Eq. (21), describing the drum wall, the residence time in the airborne phase of the granules discharged at the azimuth of flight φ , $t_{\text{air}}(\varphi)$, is obtained. With this, the axial displacement in the airborne phase Z_{air} is also obtained.

$$Z_{\text{air}}(\varphi) = u_z(\varphi) \cdot t_{\text{air}}(\varphi) \quad (22)$$

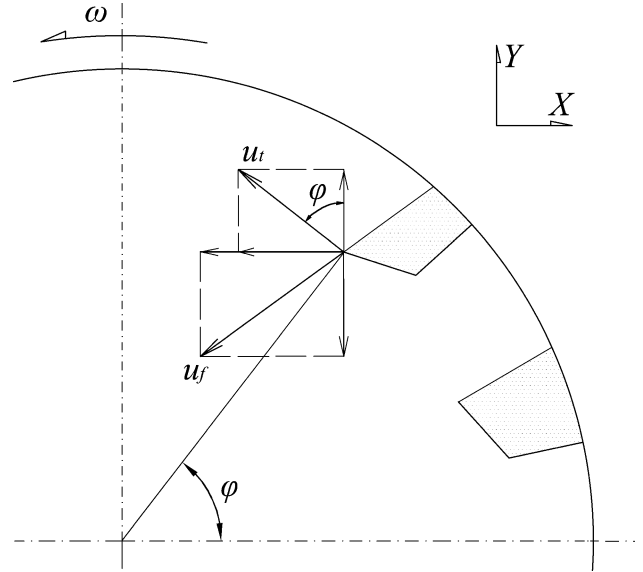


Fig. 4. Decomposition of the sliding velocity u_f and the tangential velocity u_t at the cross section of the drum (OXY plane).

2.3. The residence time and axial displacement in the dense phase

When falling into the bottom of the drum, granules enter the dense phase, and stay in dense phase until discharged. The time in the dense phase is expressed below:

$$t_{\text{dense}}(\varphi) = \beta(\varphi)/\omega \quad (23)$$

The position where the granules enter the dense phase can be obtained from the above calculation of the time in the airborne phase, and the azimuth of the position as $-\arccos((X_0 + u_x t_{\text{air}})/R')$. Since the granules are lifted by the coming flight at this position, the range of motion of the granule in the dense phase $\beta(\varphi)$ is given as the following expression [1].

$$\beta(\varphi) = \arccos((X_0 + u_x t_{\text{air}})/R') + \varphi + \frac{2\pi}{n} \quad (24)$$

As discussed above, the axial displacement in the dense phase consists of two parts, Z_{dis} and Z_{non} , and the time when the granules slide out in the flight is short and negligible compared to the circulation time. The hatched part in Fig. 3 is the amount of granules discharged in an infinitesimal time. The projection of the average displacement of the granules discharged in an infinitesimal time on the drum cross section is $(2/3)l$, therefore, the expression of $Z_{\text{dis}}(\varphi)$ is:

$$Z_{\text{dis}}(\varphi) = \frac{2}{3} l(\varphi) \cdot \tan\gamma \quad (25)$$

The length of the exposed surface of granules in a flight l depends on the pile state of granules. A polar coordinate is introduced in Fig. 3. The origin of the polar coordinate is located on the tip of the flight, the initial direction of the polar coordinate is along the flight, and the coordinate is fixed on the flight, i.e. it is rotating with the drum. It is obvious that the included angle δ , which is formed by the exposed surface of

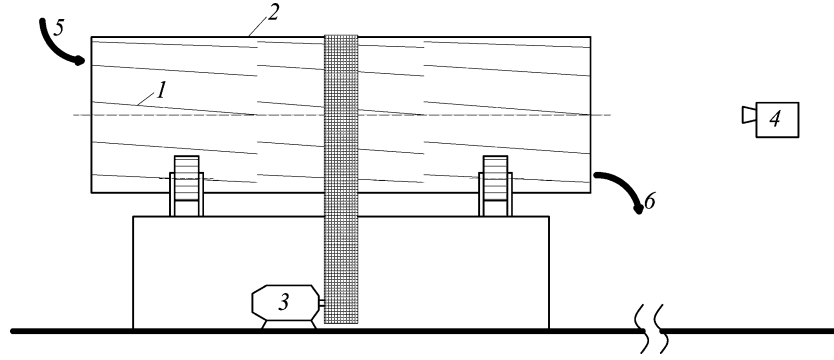


Fig. 5. Experimental apparatus 1. Flight; 2. Drum; 3. Motor; 4. Camera; 5. Feeding; 6. Flow out.

granules and the initial direction of the coordinate, depends on the azimuth of flight φ , and the following dependence is derived:

$$\delta = \psi' + \pi - \varphi - (\alpha - \arcsin(b_1 \cdot \sin(\pi - \alpha)/R')) \quad (26)$$

In the polar coordinate, the equations of flight and drum wall are shown below,

$$\begin{cases} \delta_0 = \arctan\left(\frac{b_2 \sin(\pi - \alpha)}{b_2 \cos(\pi - \alpha) + b_1}\right); \\ l \cdot \sin \delta = \tan(\pi - \alpha)(l \cdot \cos \delta - b_1); \delta \leq \delta_0 \\ l^2 + l \cdot 2R' \cdot \sin(\pi + \arcsin(b_1 \cdot \sin(\pi - \alpha)/R') - \alpha - \delta) + (R'^2 - R^2) = 0; \delta > \delta_0 \end{cases} \quad (27)$$

where δ_0 is the angle of the exposed surface of granules and the initial direction of the coordinate where the exposed surface of granules meets the line joining the flight and the drum. Therefore, the length l at any azimuth, i.e. $l(\varphi)$, is obtained from the simultaneous Eqs. (26) and (27). Introducing $l(\varphi)$ into Eq. (25), the axial displacement during discharging $Z_{\text{dis}}(\varphi)$ is obtained, and the discharging rate of a flight at any azimuth $D_{\text{dis}}(\varphi)$ is also obtained by introducing $l(\varphi)$ into Eq. (6).

According to the method Sherritt et al. [1] used to deal with granule displacement in a non-discharging process, the following assumptions are made: (1) the displacement in the non-discharging process occurs in the range of azimuth from $-(\varphi_{\text{min}} + 2\pi/n)$ to φ_{min} , as shown in Fig. 1; (2) the length of the exposed surface of granules in the flight in a non-discharging process is equal to $l(\varphi_{\text{min}})$; (3) the dynamics and

expression of the axial displacement in a non-discharging process are both similar to the axial displacement in a discharging process. With the assumptions above and some conclusions from the work of Sherritt, the non-discharging axial displacement during the time of rotating through an infinitesimal angle $d\varphi$ and the amount of granules the displacement occurs on, A_{non} , are obtained.

$$\begin{cases} Z_{\text{non}} = \frac{2}{3} l(\varphi_{\text{min}}) \cdot \tan \gamma \\ A_{\text{non}} = \int_{-(\varphi_{\text{min}} + 2\pi/n)}^{\varphi_{\text{min}}} \frac{1}{2} \left(\frac{1}{2} l(\varphi_{\text{min}}) \right)^2 d\varphi \\ = \frac{1}{2} \left(\frac{1}{2} l(\varphi_{\text{min}}) \right)^2 \cdot (2 \cdot \varphi_{\text{min}} + 2\pi/n) \end{cases} \quad (28)$$

Since Z_{non} is contributed from just a part of the granules, the average axial displacement during non-discharging of all granules \bar{Z}_{non} can be expressed as the following expression:

$$\bar{Z}_{\text{non}} = Z_{\text{non}} \cdot \frac{A_{\text{non}}}{A_{\text{max}}} \quad (29)$$

3. Verification experiments

The horizontal drum is made of polymethyl methacrylate, the radius R is 187 mm, and the length L is 1200 mm. There are three sections of flights set on the wall of the drum. In each

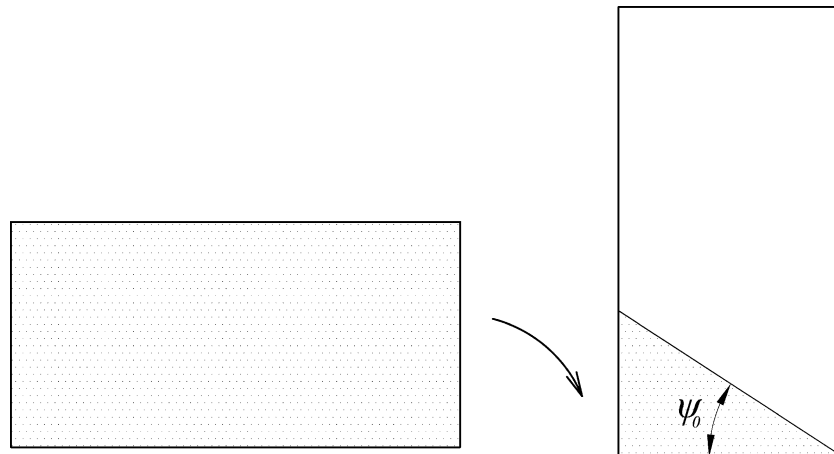


Fig. 6. Measurement of the angle of repose in the static state.

Table 1
Experimental data and model calculation

Run no.	Flight slope θ ($^\circ$)	Rotary speed N (rpm)	The initial azimuth of discharging φ_{\min} ($^\circ$)	Feed rate F (kg/min)	Calculated residence time τ (s)	Measured residence time τ (s)	Relative deviation (%)
1	3.2	5	59	0.42	685	711	-3.7
2		7	55	0.42	541	486	11.4
3		7	45	0.70	594	528	12.5
4		9	54	0.70	448	463	-3.3
5		9	42	1.05	492	466	5.7
6	5.3	3	41	0.42	794	774	2.6
7		5	36	0.70	497	537	-7.4
8		5	5	1.05	457	512	-10.8
9		7	40	1.05	362	412	-12.0
10		7	8	1.40	343	409	-16.2
11		9	34	1.40	300	356	-15.6
12	7.2	3	54	0.42	521	543	-4.1
13		5	53	0.70	327	387	-15.6
14		5	20	1.05	357	371	-3.9
15		7	46	1.05	257	315	-18.4
16		7	23	1.40	265	300	-11.7
17		9	48	1.40	207	261	-20.6

section of flights, 12 trains of folded flight are uniformly fixed around the inner wall of the drum. The widths of two segments of the folded flight, b_1 and b_2 , are both 30 mm, and the fold angle α is 125° . The slope of flight relative to the generatrix of the drum wall θ is adjustable. The rotating speed of the drum is controlled by a frequency inverter. The schematic diagram of the experimental apparatus is shown in Fig. 5.

For the application of the drum in fertilizer granulation and coating, large granules of urea with a diameter of 3 mm are used as the granules in the experiments. The angle of repose is measured by a discharge method. As shown in Fig. 6, an open box is filled with urea granules. Revolving the box slowly, let the granules discharge freely until the box is upright. When the exposed surface of the granules is steady, the static angle of repose and the coefficient of static friction are obtained by measuring the height of exposed surface. The static angle of repose of the urea granules ψ_0 is measured as 30° , i.e. the coefficient of static friction is $\tan(30^\circ)$. The coefficient of dynamic friction is substituted for with the coefficient of static friction in the model calculation.

A ruler was set on a flight as the reference, and a camera was used to record the sliding of granules out from the flight. The sliding velocity was measured by comparing the graphs for a fixed time interval. In most of the experiments, the sliding velocities of the granules u_f were nearly the same and about 188 mm/s which is used in the model calculation. The moving behavior of the granules was recorded by the camera set on the axis of drum, and the initial azimuth φ_{\min} was obtained from the graphs.

In the experimental procedure, granules were fed into the drum at a steady rate, and the granules discharged were collected and weighed at one minute intervals. When the drum was in steady state, i.e. the rate of granules discharged was equal to the feeding rate, and the feeding was stopped. The granules held in the drum were discharged out and weighed. Dividing the holdup of the drum by the feed rate, F , the mean residence time was obtained. The mean residence time was

measured in experiments with different operation parameters (ω & F) and equipment parameter (θ).

4. Analysis and discussion

The experimental parameters and mean residence times from experimental measurement and model calculation are shown in Table 1. The comparison of the measured and calculated mean residence times is shown in Fig. 7. According to Table 1 and Fig. 7, the deviations in most of the experiments are in the range $\pm 20\%$. It can be seen that the calculated mean residence times match the measured times very well, in Fig. 7. Consequently, under most of the conditions, the calculated data have a similar trend as the experiments. As an example, the calculated data are close to the curve fitted from the experimental data, as shown in Fig. 8.

Fig. 8 shows the variation of the mean residence time with the rotating speed, ignoring the effect of the feed rate. According the figure, the mean residence time follows a inverse power law with the rotating speed, which is similar to

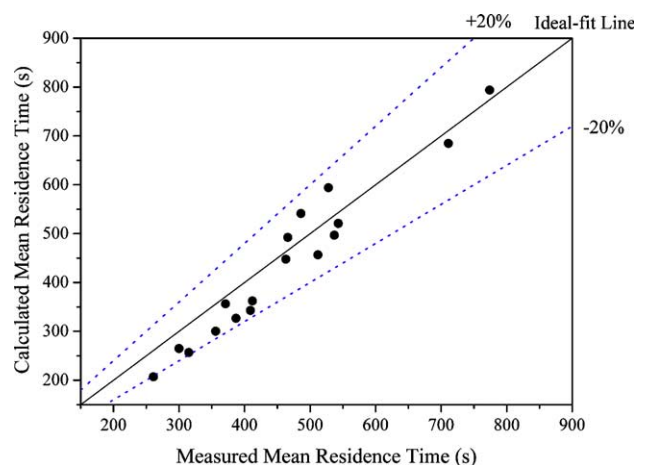


Fig. 7. Comparison of measured and calculated mean residence time.

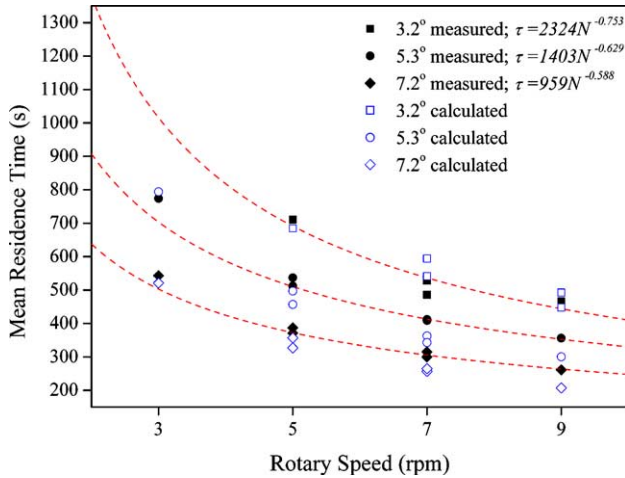


Fig. 8. Mean residence time vs. rotation speed.

the conventional drum [13]. By fitting the measured data, the indexes are -0.588 , -0.629 , -0.753 , for flight slopes at 7.2° , 5.3° , 3.2° .

As shown in Fig. 9, the influence of the feed rate on the mean residence time is small. Most of the mean deviations of the mean residence times under different conditions of the feed rate are less than 2.5%. The largest is only 4.14%. This shows that the feed rate has a small effect on the mean residence time of the granules in the drum.

It is obvious that the mean residence time increases with a decrease of flight slope. Additionally, it is expected that the mean residence time will increase much faster when the slope of the flight is closer to zero. It is shown in Fig. 10, In the condition of $\theta = 3.2^\circ$ and $N = 3$ rpm, the holdup of whole drum is larger than the maximal holdup of the drum in underloaded state even the feed rate is small. The drum in this situation is always in overloaded loading state, which is out of the range of this paper. There are only two data points for $N = 3$ rpm in experiments. It does not show sense to do a linear fit for the two data points at $N = 3$ rpm, so the data for $N = 3$ rpm are not illustrated in Fig. 10. However, that the mean residence times change approximately linearly with flight slopes. The reason

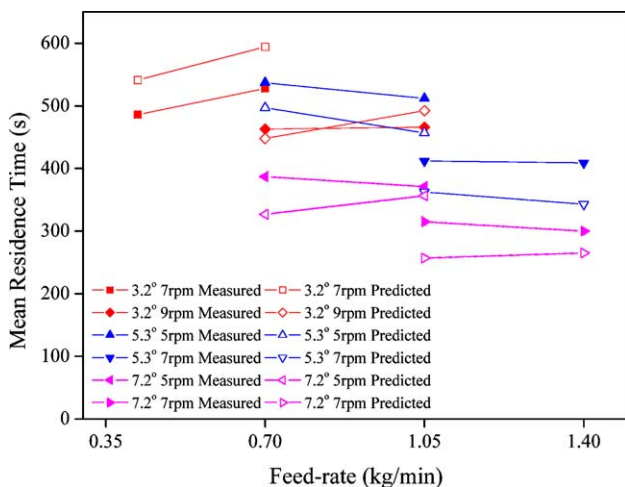


Fig. 9. Mean residence time vs. feed rate.

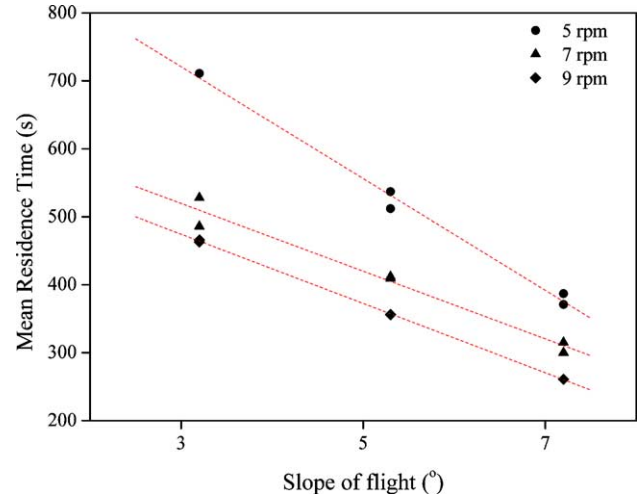


Fig. 10. Mean residence time vs. slope of the flight.

for this phenomenon may be that the derivative of the mean residence time variation is too small in the experiment range of flight slope. As expected, when the flight slope becomes smaller, the accelerated increase of the mean residence time would be obvious.

5. Conclusion

Experiments showed that granules can be steadily transported in a rotary horizontal drum with inclined flights. A mean residence time model was developed from an analysis of the granule motion. The model matches experimental results very well. The changes shown by calculated and measured data are similar. Most of the deviations between calculated and measured data are less than 20%. The experimental results showed that the feed rate has a very small influence on the mean residence time, the relationship between the mean residence time and the slope of the flight is approximately inversely proportional in the experimental range of flight slope, and the rotation speed affects the mean residence time in a minus exponential way, which is similar to the conventional inclined drum.

Nomenclature

Latin letters

- A Area of cross section of granules in a flight, which denotes the amount of granules in a flight, mm^2
- A_{non} Amount of granules contributing the non-discharging axial displacement, mm^2
- D_{dis} Discharging rate of a flight, mm^2/rad
- b_1, b_2 Width of two segments of the flight, mm
- F Feed rate of granules, kg/min
- g Acceleration of gravity, mm/s^2
- L Length of drum, mm
- l Length of the intersection of the exposed surface of granules and drum cross section, mm
- N Rotation speed of drum, rpm
- n Number of flights in the drum cross section, —
- t Circulation time of a granule, s

t_{air}	Residence time in the airborne phase, s
t_{dense}	Residence time in the dense phase, s
\bar{t}	Average circulation time for all granules, s
R	Radius of drum, mm
R'	Radius of the circle on which the tips of flights are located, mm
\bar{U}	Average speed of axial transfer, mm/s
u_t	Tangential velocity at the tip of a flight, mm/s
u_f	Sliding velocity of granules along the exposed surface, mm/s
Z	Axial displacement of granule in one circulation, mm
Z_{air}	Axial displacement in the airborne phase, mm
Z_{dis}	Axial displacement during discharging, mm
Z_{non}	Axial displacement which occurs in non-discharging, mm
\bar{Z}	Average axial displacement for all granules, mm
\bar{Z}_{non}	Average contribution to all granules from the axial displacement in non-discharging, mm

Greek letters

α	Fold angle of two segments of flight, rad
β	Angle of the granule in the dense phase, rad
γ	Shift angle, the direction at which granules slide relative to the drum cross section, rad
δ	Included angle of the exposed surface of granules relative to the initial direction of the polar coordinate, rad
θ	Slope of flights relative to the generatrix of drum wall, rad
φ	Azimuth of flight, rad
φ_{max}	Azimuth of flight at the end of the flight discharging process, rad
φ_{min}	Azimuth of flight at the start of the flight discharging process, rad
ψ	Kinetic angle of repose, i.e. the included angle formed by the exposed surface of granules and horizontal plane when the drum is in motion, rad
ψ_0	Static angle of repose, i.e. the include angle formed by the exposed surface of granules and the horizontal plane in the static state, rad
ψ'	Included angle formed by the horizontal plane and the intersection of the drum cross section and the exposed surface of granule, rad

τ	Mean residence time of granules, s
μ	Kinetic friction coefficient, –
ω	Rotation speed of drum, rad/s

Acknowledgment

The authors wish to express their appreciation for the financial support of this study by the fundamental research project from China Petroleum and Chemical Corporation (Sinopec Corp). The grant number is No. X502025.

References

- [1] Richard G. Sherritt, Rod Caple, Leo A. Behie, Anil K. Mehrotra, The movement of solids through flighted rotating drums. Part I: Model formulation, *Canadian Journal of Chemical Engineering* 71 (6) (1993) 337–346.
- [2] Harvey M. Goertz, Richard J. Timmons, George, R. McVey, Sulfur coated fertilizers and process for the preparation. US Patent: 5219465. 1993.
- [3] Ting-Jie Wang, Yong Jin, Fei Wei, Jing-Fu Wang, Zhan-Wen Wang. A granulation methods and device with a fluidized bed in a drum, China patent. 02146785.4, 2002.
- [4] W.C. Saeman, Passage of solids through rotary kilns. Factor affecting time of passage, *Chemical Engineering Progress* 47 (10) (1951) 508–514.
- [5] F.Y. Wang, I.T. Cameron, J.D. Litster, P.L. Douglas, A distributed parameter approach to the dynamics of rotary drying processes, *Drying Technology* 11 (7) (1993) 1641–1656.
- [6] F.Y. Wang, I.T. Cameron, J.D. Litster, Further theoretical studies on rotary drying processes represented by distributed systems, *Drying Technology* 13 (3) (1995) 737–751.
- [7] F.Y. Wang, I.T. Cameron, J.D. Litster, V. Rudolph, A fundamental study on particle transport through rotary dryers for flight design and system optimisation, *Drying Technology* 13 (5–7) (1995) 1261–1278.
- [8] D. Revol, D.L. Briens, J.M. Chabagno, The design of flights in rotary dryers, *Powder Technology* 121 (2001) 230–238.
- [9] Wenzhou Wang, Three-arc lifting flight, *Journal of Chemical Industry and Engineering (China)* 51 (4) (2000) 446–451.
- [10] R.Y. Yang, R.P. Zou, A.B. Yu, Microdynamic analysis of particle flow in a horizontal rotating drum, *Powder Technology* 130 (2003) 138–146.
- [11] Y.L. Ding, R. Forster, J.P.K. Seville, D.J. Parker, Segregation of granular flow in the transverse plane of a rolling mode rotating drum, *International Journal of Multiphase Flow* 28 (2002) 635–663.
- [12] F.R. Schofield, P.G. Glikin, Rotary driers and coolers for granular fertilizers, *Institution of Chemical Engineers—Transactions* 40 (3) (1962) 183–190.
- [13] P.S.T. Sai, G.D. Surender, A.D. Damodaran, V. Suresh, Z.G. Philip, K. Sankaran, Residence time distribution and material flow studies in a rotary kiln, *Metallurgical Transactions. B, Process Metallurgy* 21 (6) (1990) 1005–1011.